


Received: 17 December 2021

Accepted: 2 January 2022

# Enzyme based amperometric wide field biosensors: Is single-molecule detection possible?

Angelo Tricase<sup>1,‡</sup> | Anna Imbriano<sup>1,4,‡</sup> | Eleonora Macchia<sup>2</sup> | Lucia Sarcina<sup>1</sup> | Cecilia Scandurra<sup>1</sup> | Fabrizio Torricelli<sup>3</sup> | Nicola Cioffi<sup>1,4</sup> | Luisa Torsi<sup>1,2,4</sup> | Paolo Bollella<sup>1,4</sup> 

<sup>1</sup> Dipartimento di Chimica, Università degli Studi di Bari "Aldo Moro", Bari, Italy

<sup>2</sup> Faculty of Science and Engineering, Åbo Akademi University, Turku, Finland

<sup>3</sup> Dipartimento Ingegneria dell'Informazione, Università degli Studi di Brescia, Brescia, Italy

<sup>4</sup> Centre for Colloid and Surface Science, Università degli Studi di Bari "Aldo Moro", Bari, Italy

## Correspondence

Paolo Bollella and Luisa Torsi, Dipartimento di Chimica, Università degli Studi di Bari "Aldo Moro", 70125 Bari, Italy.  
 Email: [paolo.bollella@uniba.it](mailto:paolo.bollella@uniba.it) and [luisa.torsi@uniba.it](mailto:luisa.torsi@uniba.it)

<sup>‡</sup>These authors contributed equally to this work.

## Funding information

Academy of Finland projects, Grant/Award Numbers: 316881, 316883; Spatiotemporal control of Cell Functions, Grant/Award Numbers: 332106, 6CDD3786; SiMBiT, Grant/Award Number: 824946

## Abstract

This review discloses the technological advances involving enzyme-based amperometric biosensors engaging challenging limits of detection as low as a single molecule. At first, we summarise the most recent findings concerning electrode modification toward the enhancement of the enzyme loading accomplished mainly through the deposition of nanomaterials. The increase of the electron transfer (ET) rate is mostly based on the enzyme site-specific immobilization through the analysis of the enzyme structure/sequence and protein bioengineering is overviewed. However, both approaches are not appropriate to develop enzyme-based amperometric biosensors able to reach reliable analytical detections below micro-/nano-molar. The last part is devoted to single-molecule electrochemistry that has been widely exploited as a near-field approach in the last decades as a proof-of-concept for the detection of single ET events. Organic electrochemical transistors operated as Faradaic current amplifiers do not detect below micro-/nano-molar. We here propose an alternative approach based on the combination of an electrochemical cell with a bipolar junction transistor in the extended base configuration, drawing some conclusions and future perspectives on the detection of single ET events at a large electrode for the development of Point-of-Care devices.

## KEYWORDS

bipolar junction transistor, enzymatic recycling, modified electrodes, redox enzymes, single-molecule electrochemistry

**Abbreviations:** BC, base and collector; CDH, cellobiose dehydrogenase; CNTs, carbon nanotubes; CYT, cytochrome domain; DET, direct electron transfer; EB, emitter and base; EDC, 1-ethyl-3-(3-dimethylaminopropyl)carbodiimide; ET, electron transfer; FAD, flavin adenine dinucleotide; FDH, fructose dehydrogenase; GCE, glassy carbon electrode; GOx, glucose oxidase; h-PG, highly porous gold electrode; HRP, horseradish peroxidase; IET, internal ET; LOD, limit of detection; LOQ, limit of quantification; MWCNTs, multiwalled CNTs; NHS, N-hydroxysuccinimide; OECTs, organic electrochemical transistors; PEI, polyethyleneimine; PGE, pyrolytic graphite 'edge'; pI, isoelectric point; PoC, point-of-care; SWCNTs, single-walled CNTs

This is an open access article under the terms of the [Creative Commons Attribution](https://creativecommons.org/licenses/by/4.0/) License, which permits use, distribution and reproduction in any medium, provided the original work is properly cited.

© 2022 The Authors. *Electrochemical Science Advances* published by Wiley-VCH GmbH.

## 1 | INTRODUCTION

Enzyme-based amperometric biosensors have been at the forefront of electrochemical technologies in the last six decades considering the evolution from the classical electrochemical cell to screen printed electrodes for in situ measurements till nowadays wearable and e-textile amperometric biosensors toward the continuous and remote healthcare.<sup>[1–5]</sup> The electron transfer (ET) mechanism can be classified as follows,<sup>[6]</sup> (Figure 1): (i) first generation where O<sub>2</sub> is working as a primary electron acceptor toward substrate oxidation, hence the consumption of O<sub>2</sub> with Clark's electrode or the production of H<sub>2</sub>O<sub>2</sub> with a solid electrode (e.g., carbon-based electrode, Prussian blue modified electrode, etc.) can be used,<sup>[7,8]</sup> the second generation where a free-diffusing or immobilized mediator is shuttling electrons directly from the active center of the enzyme or re-oxidizing the enzymatic cofactor (e.g., pyrroloquinoline quinone oxidizing nicotinamide adenine dinucleotide back to NAD<sup>+</sup>),<sup>[9–11]</sup> and the third generation where electrons can be directly transferred from the active center to the electrode.<sup>[12–14]</sup>

Despite the definition, not all enzymes are able to perform direct ET (DET) to the electrode most probably due to their large dimensions (above ~18 Å), active redox center (prosthetic group) deeply buried in the enzyme scaffold, and a high degree of glycosylation.<sup>[15,16]</sup> The ET rate decreasing, due to enzyme dimensions larger than the Marcus ET maximum distance and deeply buried prosthetic groups, can be mathematically demonstrated by recalling the ET theory from Marcus.<sup>[17–21]</sup> In biological systems, the distance between the electrons donor (D)-acceptor (A) affects the ET rate. Accordingly, ET can be calculated as follows:

$$k_{ET} \propto e^{[-\beta(d-d_0)]} e^{\left[ \frac{-(\Delta G^0 + \lambda)^2}{4RT\lambda} \right]} \quad (1)$$

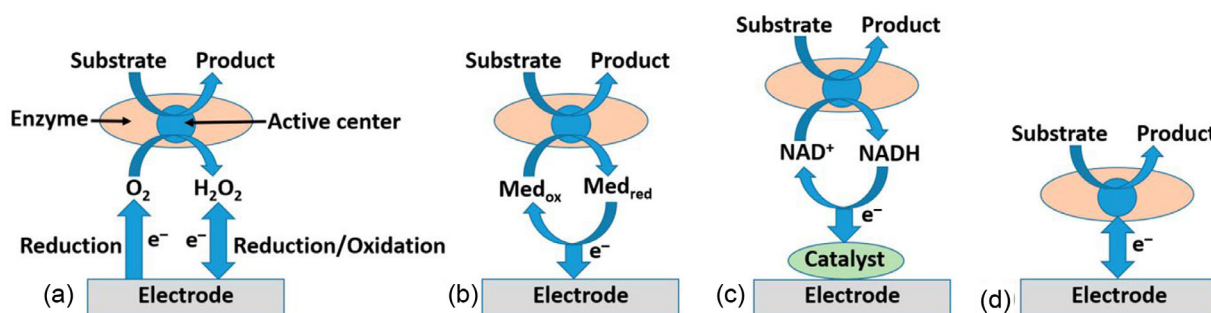


**FIGURE 1** Different electron transfer (ET) pathways: (a) ET through electroactive enzyme-substrate/product (herein shown as monitoring O<sub>2</sub> reduction or H<sub>2</sub>O<sub>2</sub> oxidation/reduction). (b) ET through freely diffusing or immobilized electron relays (defined as redox mediators). (c) ET through catalysts able to oxidize nicotinamide adenine dinucleotide (NADH) produced upon the enzymatic reaction from NAD<sup>+</sup>. (d) Direct ET also defined as direct ET (DET) between the enzyme redox center and the electrode surface. Reprinted<sup>[2]</sup> with permission of MDPI AG under the <https://creativecommons.org/licenses/by/4.0/>

where  $\beta$  corresponds to the decay or attenuation factor (about 10 nm<sup>-1</sup> for proteins),  $\Delta G^0$  and  $\lambda$  correspond to the free Gibbs energy and reorganization energy accompanying the ET process,  $d_0$  and  $d$  are the Van der Waals distance and the actual distance between the redox-active site and the electrode, while  $R$  and  $T$  have their usual meanings.<sup>[22]</sup> Hence, the ET rate constant can be approximated as  $e^{-\beta r}$ , exponentially depending on the distance between D and A (as reactants). However, the ET rate constant depends also on intrinsic ( $\lambda$ ) and thermodynamic ( $\Delta G^0$ ) factors as well as from the mutual orientation of the reactants. The upper limit of approximately 18 Å was experimentally demonstrated by Yaropolov and his co-workers,<sup>[23,24]</sup> who investigated the ET mechanism of laccase by presorbing lipid layers with different thicknesses. The efficiency of electrocatalysis was shown to be constant up to a 20 Å distance between the enzyme molecule and the electrode surface.<sup>[25]</sup> Hence, below 18 Å the enzyme-catalyzed reaction is the limiting step in the ET process.<sup>[26,27]</sup> Regarding the enzyme glycosylation degree, Gorton and co-workers demonstrated experimentally that the removal of sugar residues from the outer shell of the enzyme, notably cellobiose dehydrogenase (CDH) from *Phanerochaete chrysosporium*, allowed to increase the ET rate.<sup>[28,29]</sup> The glycosylation was ascribed mainly to mannose-type carbohydrate chains for a total molecular weight of 1800 Da. By chopping the enzyme in specific sites, the authors were able to reduce the hydrodynamic radius by 30% (measured by dynamic light scattering measurements), consequently increasing the catalytic current by 40% (directly correlated with ET rate efficiency).

In this regard, one of the most relevant discussions in the field was the DET performed by glucose oxidase (GOx).<sup>[30]</sup> Indeed, GOx has been considered at least for three decades as an ideal redox enzyme able to directly transfer electrons to the electrode surface, as stated in a review paper

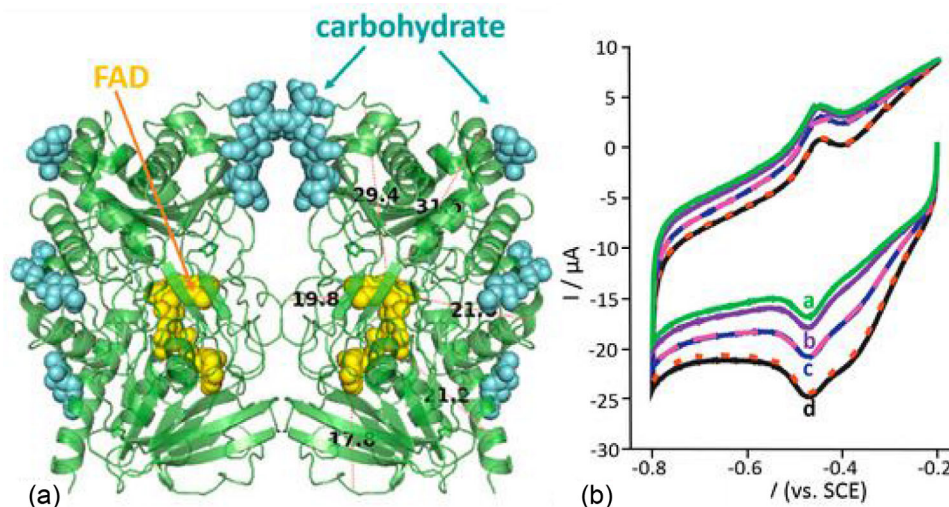


**FIGURE 2** (a) Secondary structure of glucose oxidase (GOx) available as a PDB file, PDB code 1gal <http://www.rcsb.org/pdb/explore/explore.do?structureId=1GAL>. (b) Cyclic voltammograms showing  $O_2$  reduction on a GOx/MWCNTs/GCE: (a) 0 mM, (b) 2 mM, (c) 4 mM, and (d) 8 mM glucose. Experimental conditions: 100 mM phosphate buffer, pH 6.8, at a scan rate of  $60 \text{ mV s}^{-1}$ . Reproduced<sup>[34]</sup> with permission of Elsevier Ltd

in 1992.<sup>[31]</sup> Recently, the group of redox enzymes able to perform DET has been restricted to 50 among 3500.<sup>[28]</sup> In 2016, Wilson briefly summarised in an editorial the reasons why native GOx cannot undergo DET despite the huge numbers of papers reporting it.<sup>[32]</sup> Although flavin adenine dinucleotide (FAD) cofactors are not covalently bound to the enzyme scaffold, a clear couple of redox peaks with a formal potential at pH 7 of about  $-0.45 \text{ V}$  versus Ag/AgCl (3 M KCl, all potentials are reported toward this reference if not otherwise stated) was observed in many modified electrodes with ET rate constants in the range  $1\text{--}10 \text{ s}^{-1}$ . At this point, a spontaneous question is arising about the origin of these peaks. However, Wooten et al. demonstrated the peaks of freely diffusing FAD and presumably GOx-modified electrode were occurring exactly at the same potential.<sup>[33]</sup> The origin of FAD cannot be elucidated by conventional cyclic voltammetry, but eventually considering redox titration one can extrapolate the formal potential for the bound and freely diffusing FAD,  $-0.302$  and  $-0.417 \text{ V}$ , respectively. The freely diffusing FAD is unable to oxidize glucose, thus no oxidative (or anodic) catalytic wave will be observed. This is unfortunately displayed in many published papers as a misunderstanding of the recorded cyclic voltammograms. Afterward, Bartlett and Al-Lolage unequivocally demonstrated the absence of DET from GOx immobilized onto multiwalled carbon nanotubes (MWCNTs) modified electrodes.<sup>[34]</sup> In this case, the authors used a mix of L-glucose and D-glucose (with different concentrations) to prove that the reduction wave clearly visible for a GOx modified electrode can be ascribed to  $O_2$  reduction to  $H_2O_2$ , as shown in Figure 2.

They observe a decreasing of the catalytic current only with the addition of D-glucose that can be enzymatically converted to gluconic acid with the contemporary consumption of  $O_2$  (to produce  $H_2O_2$  by GOx conversion) while L-glucose cannot be processed. Notably, the smaller catalytic current is mainly due to the decreasing of the amount of dissolved  $O_2$  available for its non-enzymatic reduction occurring at the electrode surface (faster kinetics). Unfortunately, most of the claims supported by the sentence “the data presented are similar to previously reported literature”, were successfully published without considering the reliability of the collected data.<sup>[2]</sup>

Besides the historical debate on DET of GOx (still open at certain extends), this review aims at reviewing the most popular strategies that have been used to improve the amperometric responses of enzyme-based biosensors devoting particular attention to the modification of electrodes with nanomaterials (e.g., carbon-based nanomaterials, metal nanoparticles, redox polymers, conducting polymers, layer-by-layer architecture) toward enzyme loading enhancing.<sup>[35–38]</sup> In addition, electrode modifications based on enzyme orientation and site-specific wiring will be summarized based on structural consideration of enzymes (e.g., the presence of hydrophobic pockets or the insertion of particular functional groups on the enzyme surface through enzyme bioengineering).<sup>[39–41]</sup> Furthermore, this review aims at unraveling the possibility to amplify the amperometric response of enzyme-based biosensors by combining electrochemical platforms and bipolar junction transistors (BJT) toward single-molecule electrochemistry, so far proposed only as a near-field approach.<sup>[42–45]</sup> This amplification of at least 2–3 orders of

magnitude combined with the enzymatic recycling carried out by  $10^{11}$ – $10^{12}$  bioreceptors on large-area electrodes could potentially pave the way for the development of highly sensitive enzyme-based biosensors able to detect metabolites in concentrations as low as in the nanomolar range or sub-nanomolar range ( $< \text{nM}$ ) down to the single molecule, opening their applications toward the clinically relevant biomarkers' early detection. Such kind of biosensors would be particularly needed for the early and continuous monitoring of metabolites/biomarkers related to neurodegenerative diseases but also healthcare-associated infections and many other diseases. Finally, the review will compare this new 'amplification' route with the ones previously pursued providing some perspectives for future research within the field.

## 2 | ENHANCING THE AMPEROMETRIC RESPONSE OF ENZYME-BASED BIOSENSORS

The improvement of sensitivity, as well as other analytical figures of merit (e.g., the limit of detection [LOD], the limit of quantification [LOQ], selectivity, etc.), has been the core aspect of the research performed about enzyme-based amperometric biosensors.<sup>[46,47]</sup> Researchers focused their attention mainly in two directions: (i) increasing the enzyme loading and (ii) improving the ET rate.<sup>[48–51]</sup> However, we should stress the concept that increasing the enzyme loading will have a small effect on LOD, but it will heavily affect the dynamic linear range, especially considering the definition of the enzymatic electrocatalytic current ( $I_{el}$ )<sup>[52]</sup> resulting from the mass-transfer-limited current,  $I_{lim}$ ; the kinetically limited current,  $I_{kin}$ ; and  $I_E$ , the current related to the interfacial ET:

$$\frac{1}{I_{el}} = \frac{1}{I_{lim}} + \frac{1}{I_{kin}} + \frac{1}{I_E} \quad (2)$$

$I_{lim}$  accounts for the diffusion of the substrate from the bulk solution toward the enzyme-modified electrode (investigated by using rotating disk electrode, Koutecky–Levich plot with  $1/I_{lim}$  vs.  $\omega^{-1/2}$ ):<sup>[53]</sup>

$$I_{lim} = 0.620nF [C] D^{2/3} A \nu^{-1/6} \omega^{1/2} \quad (3)$$

where  $n$  is the number of electrons,  $F$  is the Faraday's constant  $96485 \text{ C mol}^{-1}$ ,  $[C]$  is the concentration of substrate,  $D$  is the diffusion coefficient of the substrate,  $A$  is the area of the electrode,  $\nu$  is the kinetic viscosity of the electrolyte and  $\omega$  is the rotation rate per minute in rpm.  $I_{kin}$  accounts for the catalytic properties defined according to the Michaelis-

Menten equation:

$$I_{kin} = \frac{nFA\Gamma k_{cat} [C]}{[C] + K_M} \quad (4)$$

where  $n$ ,  $F$ ,  $[C]$ , and  $A$  have their usual meanings,  $k_{cat}$  is the turnover number for the enzymatically catalyzed reaction ( $\text{s}^{-1}$ ),  $\Gamma$  is the enzyme surface coverage normalized by the electrode area ( $\text{mol cm}^{-2}$ ) and  $K_M$  is the Michaelis-Menten constant ( $\text{mM}$ ).<sup>[54,55]</sup>  $I_E$  accounting for the ET rate can be derived from the Butler-Volmer equation:

$$I_E = nFA\Gamma k_s \quad (5)$$

where  $n$ ,  $F$ ,  $A$ , and  $\Gamma$  have their usual meanings and  $k_s$  is the heterogeneous ET rate constant.<sup>[56]</sup>

In Equations (4) and (5), it is possible to observe the direct proportionality of both current contributions ( $I_{kin}$  and  $I_E$ ) toward the surface coverage ( $\Gamma$ ), thus by increasing the enzyme loading we can enhance the amperometric output response of enzyme-based biosensors possibly extending the upper limit of the dynamic linear range (anyway limited at very high substrate concentrations by enzyme saturation).

Alternatively, many researchers considered the possibility to insert some functional groups that would allow for the site-specific binding in the proximity of redox-active groups directly involved both in catalytic processes and in ET. In addition, the presence of hydrophobic pockets or cysteine residues (unfortunately not exposed on the outer surface of the enzyme) would allow for an enzyme plugging or wiring excluding random orientations that are negatively affecting  $k_s$ . This eventually can promote the detection of small substrate concentrations by increasing the ET rate.

### 2.1 | Increasing the enzyme loading

As previously mentioned, increasing the enzyme loading onto the electrode will have a small effect on LOD (usually occurring still in the  $\mu\text{M}$  range) but will extend the dynamic linear range by affecting the diffusion of the substrate toward the enzyme-modified electrode. To this extent, the electrode can be modified with metal or carbon-based nanomaterials synthesized by wet chemistry (i.e., bottom-up and top-down methods)<sup>[36]</sup> or by electrodeposition from a sacrificial solution (i.e., electrodeposition of highly porous gold from  $10 \text{ mM HAuCl}_4$  containing  $3 \text{ M NH}_4\text{Cl}$ ).<sup>[35,57,58]</sup> For instance, CNTs, both single- and multi-walled,<sup>[59,60]</sup> have been widely employed for the development of enzyme-based biosensors. In this regard,



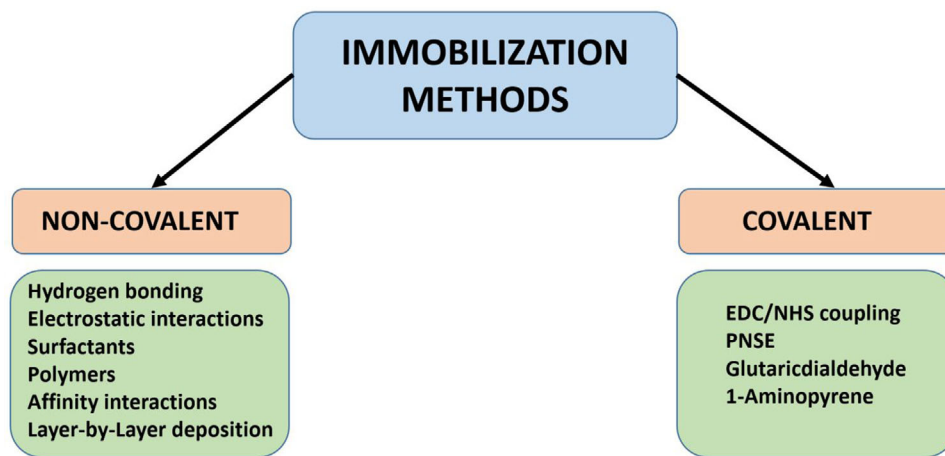


FIGURE 3 Classification of enzyme immobilization methods on carbon nanotubes (CNTs) reported in the literature. Reproduced<sup>[36]</sup> with permission of Elsevier Ltd

many functionalization protocols have been explored and are essentially divided into two groups, namely non-covalent and covalent methods, as schematically displayed in Figure 3.

Although the formers are not considered reliable immobilization methods, they tend to prevent conformational rearrangements of the enzyme structure still enhancing the surface coverage compared to non-modified electrodes.<sup>[61–63]</sup> However, we should highlight that the random orientation of the enzyme will promote several ET pathways that will not be equally efficient. Furthermore, considering the enzyme structure, the non-covalent deposition can be driven by hydrogen bonding or electrostatic interactions, and by modifying CNTs with surfactants or polymers (i.e., polyethyleneimine [PEI], poly(diallyldimethylammonium chloride), etc.). For CNTs, we need to account also for hydrophobic interactions and  $\pi$ - $\pi$  stacking between the sidewalls of CNTs and the aromatic sidechains of amino acids contained in the enzyme structure. However, the covalent methods include the modification of CNTs with 1-pyrenebutyric acid *N*-hydroxysuccinimide ester, 1-ethyl-3-(3-dimethylaminopropyl)carbodiimide/*N*-hydroxysuccinimide (EDC/NHS) covalent immobilization, glutaraldehyde cross-linking and physical entrapment through photo-polymerized molecules like poly(vinyl alcohol), *N*-methyl-4(4'-formylstyryl)pyridinium methosulfate acetal.<sup>[64]</sup>

Besides CNTs, there are several carbon-based nanomaterials that have been exploited in the last 30 years for the development of biosensors like graphene, carbon black, graphene 2-D like nanomaterials (i.e., molybdenum disulfide (MoS<sub>2</sub>), graphite-carbon nitride (g-C<sub>3</sub>N<sub>4</sub>), etc.).<sup>[65]</sup> Moreover, carbon-based nanomaterials were also combined with metal-based nanoparticles to develop hybrid

nanomaterials.<sup>[66]</sup> We will now review a few examples where the presence of carbon-based nanomaterials increased the enzyme loading devoting particular attention to the analytical figures of merit.

In the last decades, many researchers reported the combination of immobilized enzymes onto nanostructured electrodes.<sup>[67–73]</sup> Herein, we are discussing the most representative approaches. For instance, Qian and Yang reported on the influence of MWCNTs on the immobilization of horseradish peroxidase (HRP) and its loading on the electrode surface.<sup>[74]</sup> The authors cross-linked the enzyme onto MWCNTs modified glassy carbon electrode (GCE) by using chitosan. In Figure 4a, it is possible to observe as the LOD was not affected by the addition of MWCNTs while the dynamic linear range was extended. Notably, HRP/GCE exhibited a linear range between approximately 0.1 and 0.3 mM (LOD was not specified), while HRP/Chitosan/MWCNTs/GCE exhibited a linear response in the range 16.7–740  $\mu$ M with a sensitivity of 4.995  $\mu$ A mM<sup>-1</sup> and a LOD of 10.3  $\mu$ M. Moreover, Figure 4b shows the increase of the amperometric output with the increase of the amount of MWCNTs deposited onto the electrode surface probably due to the enlargement of the electroactive area with respect to the bare GCE, being directly related to the increasing of HRP loading. However, it has been demonstrated that the internal cavities and sidewalls of the CNTs can accommodate various biomolecules. This feature has inspired in coupling CNTs with GOx,<sup>[75]</sup> catalase,<sup>[76,77]</sup> cytochrome P450,<sup>[78]</sup> alcohol oxidase,<sup>[79,80]</sup> etc. Gooding et al. investigated the ET features of microperoxidase-11 conjugated onto aligned CNTs covalently linked on gold electrodes through thiol groups.<sup>[81]</sup>

Alternatively, metal-based nanoparticles have been exploited to increase the enzyme loading and preserve

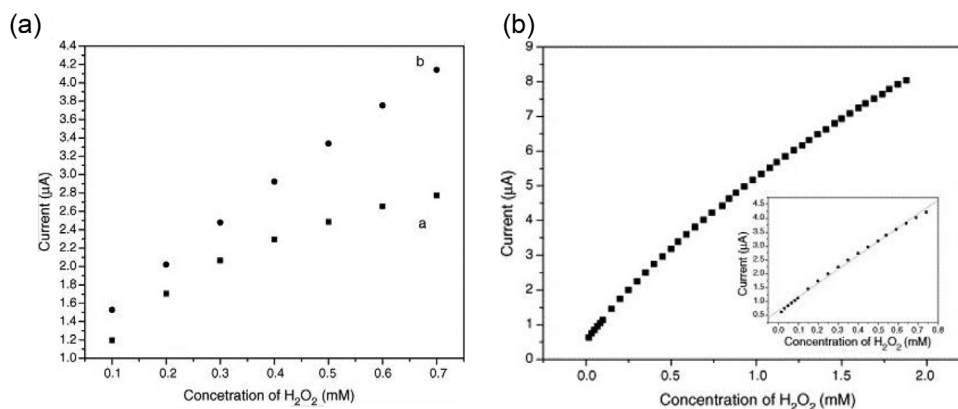


**FIGURE 4** (a) Calibration curve for the concentration of H<sub>2</sub>O<sub>2</sub> in the range of 0.1–0.7 mM in phosphate buffer solution (0.1 M, pH 6.9): applied potential,  $-0.2$  V; (a) Multiwalled nanotubes (MWNTs) coated GCE and (b) enzyme electrode. (b) Calibration curve of the enzyme electrode: applied potential,  $-0.2$  V; supporting electrolyte, 0.1 M phosphate buffer solution (pH 6.9). Insert the linear relationship between amperometric response with a concentration of H<sub>2</sub>O<sub>2</sub>. Adopted<sup>[74]</sup> with permission of Elsevier Ltd

the enzyme layer from uneven degradation processes. For example, Schulz and co-workers reported the immobilization of CDH onto gold nanoparticles modified with PEI by exploiting the electrostatic attraction between the enzyme (isoelectric point [pI]  $\sim 4.1$ , hence negatively charged at both immobilization and working pH) and the surface always positively charged.<sup>[82]</sup> In this case, the authors were able to increase the enzyme loading by several orders of magnitude (well-defined redox peak for *heme b* group) with respect to the unmodified gold electrode (peaks not visible at all). Moreover, the platform was stable considering a decrease in the catalytic response of only 5.3% considering its continuous operation under flow-injection conditions for 24 h. This stability might be ascribed to the tight electrostatic interaction between the enzyme and the positively charged gold nanoparticles.

Recently, Bollella and co-workers reported the immobilization of fructose dehydrogenase (FDH) onto a highly porous gold electrode (h-PG) prepared through the preventive electrodeposition of a sacrificial layer of gold microparticles lately undergoing hydrogen evolution reaction at the electrode responsible for the H<sub>2</sub>-bubbling at the electrode that acts as a self-template to obtain an h-PG. The so prepared electrode was further modified with self-assembled monolayers bearing different functional groups, notably -COOH, -OH, and -NH<sub>2</sub> to explore the enzyme orientation through electrostatic interaction (pI  $\sim 5.6$  according to the enzymatic sequence). In this case, we can observe the increase of the enzyme loading as well as the catalytic efficiency of the 4-mercaptophenol-modified electrode surface as depicted in Figure 5. This electrode platform retained 90% of its catalytic response after 90 days (meant as storage condition not as working stability).<sup>[83]</sup>

Besides the continuous technological advances in the field already reported, many researchers are still pursu-

ing this route sometimes even synthesizing some enzyme-mimicking nanomaterials (regarded as nanozymes) that allow increasing indefinitely the surface coverage showing promising analytical performance.

## 2.2 | Increasing the ET rate

As previously mentioned, increasing the enzyme loading might not affect the LOD but only the dynamic linear range extension. Furthermore, the normalization of all data by the electroactive area would reduce the amplification factor related to the real electrode area obtained after the deposition of nanomaterials like CNTs or metal-based nanoparticles. Alternatively, many researchers focused their work on the investigation of efficient wiring or orientation methods that would contribute to increasing the ET rate, hence the sensitivity of the enzyme-based amperometric biosensor (with LODs still in the micro-/nanomolar range).

Particularly, Patolsky et al. reported the modification of a gold electrode with thiolated CNTs to electrically wire GOx through the reconstitution of the apo-enzyme onto a FAD moiety covalently immobilized by EDC/NHS coupling, as schematically shown in Figure 6.<sup>[84]</sup>

The so modified electrode is considered one of the few examples of DET between GOx and electrode. However, we should emphasize as the author investigated the negative effect of the length of single-walled CNTs (SWCNTs) on the ET rate constant. Indeed, the ET rate constants ( $k_s$ ) were decreasing from 83 till 12 s<sup>-1</sup> by increasing the length of SWCNTs from 25 to 150 nm on average. As shown from glucose oxidation, the nanotube length indeed affects the ET between the FAD units (GOx is a dimeric enzyme) and the electrode. However, the authors did not elucidate the ET

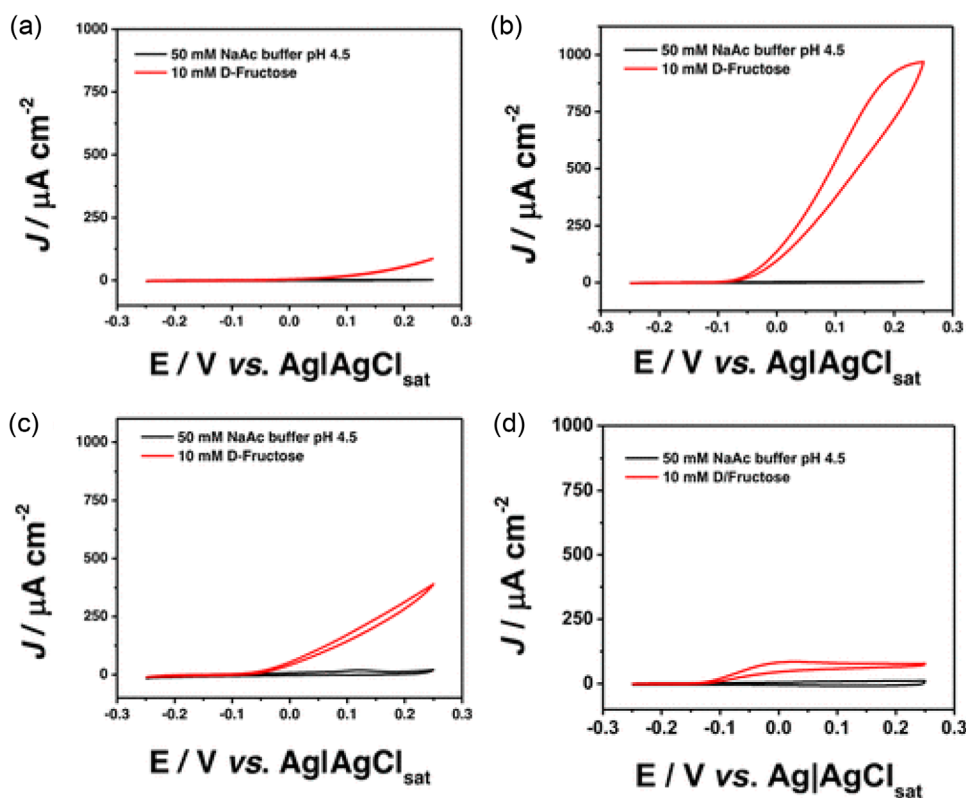


FIGURE 5 Cyclic voltammograms (CVs) of FDH/4-MBA/h-PG (A), FDH/4-MPh/h-PG (B), FDH/4-APh/h-PG (C), and FDH/h-PG (D) in the absence (black curve) and in the presence of 10 mM D-fructose (red curve). Experimental conditions: 50 mM NaAc buffer at pH 4.5, scan rate  $5 \text{ mV s}^{-1}$ ,  $T = 25^\circ\text{C}$ . Adopted<sup>[83]</sup> with permission of American Chemical Society (ACS)

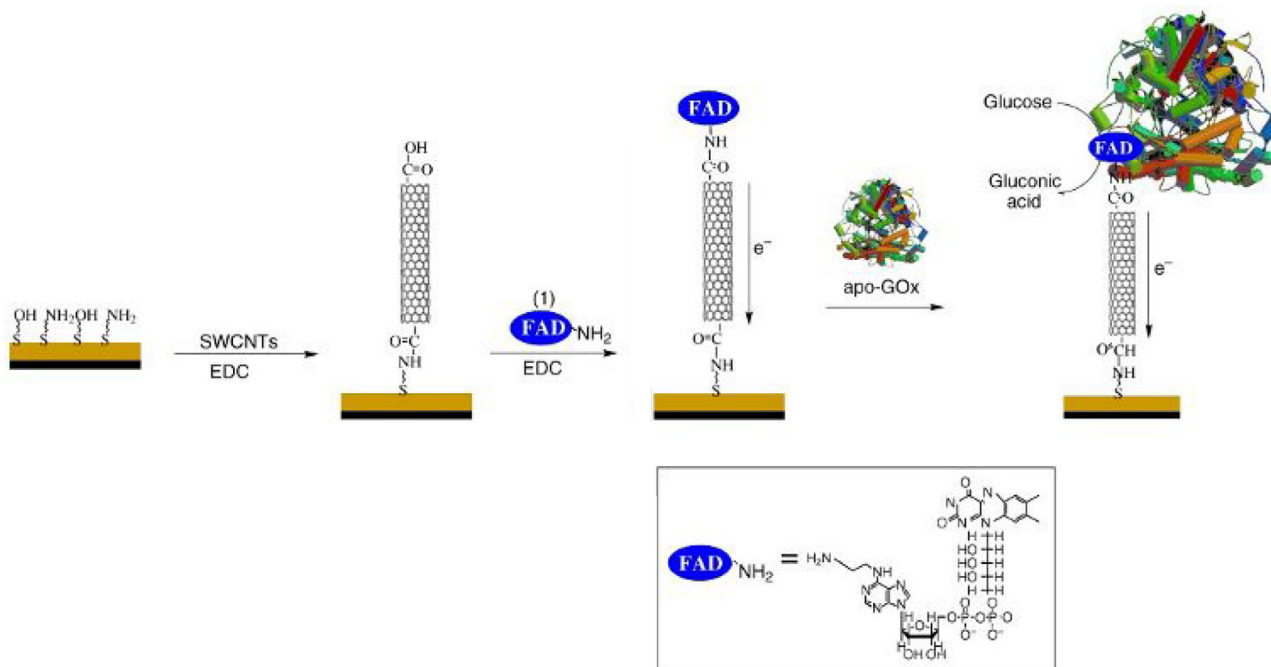
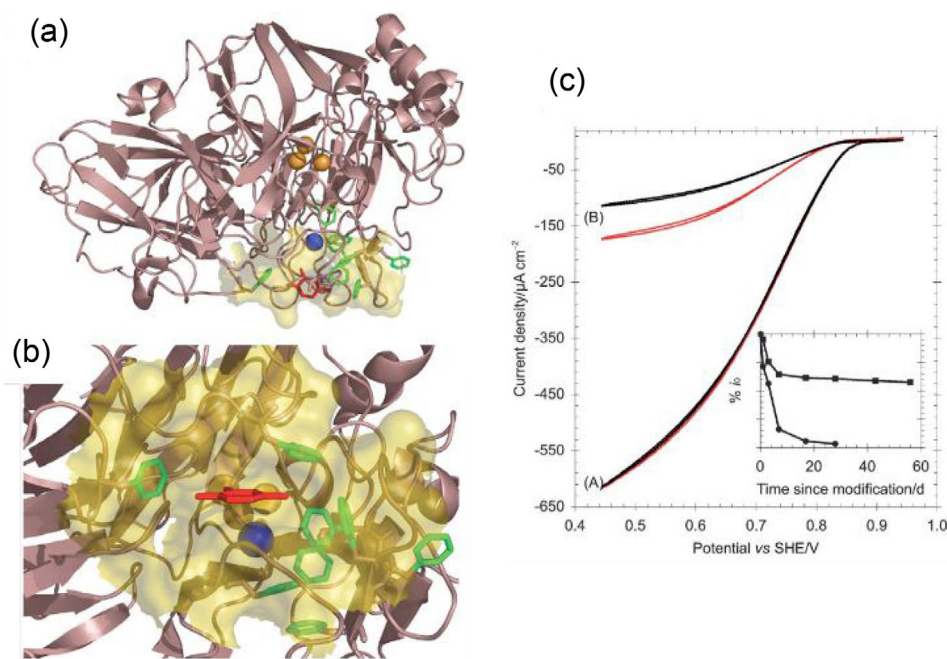


FIGURE 6 Electrical connection of glucose oxidase (GOx) on single-walled carbon nanotubes (SWCNTs). Adopted<sup>[84]</sup> with permission of Wiley



**FIGURE 7** Representations of *Trametes versicolor* laccase III (PDB code: 1KYA) (a) with the hydrophobic binding pocket. (b) Binding pocket highlighted in yellow. (c) The electrocatalytic activity of a laccase film freshly spotted (black curves) on the electrode (a) a2A/PGE and (b) an unmodified pyrolytic graphite 'edge' (PGE). The red curves are cyclic voltammograms recorded after buffer exchange (no residual enzyme in solution). Inset: Long-term stability for a modified (■) and unmodified (●) electrode. Reproduced<sup>[86]</sup> with permission of Royal Society of Chemistry (RSC)

mechanism, but the distances considered might exclude the possibility of charge transport by tunneling processes.

Considering another approach, Armstrong and co-workers demonstrated the possibility to plug an enzyme onto the electrode surface focusing their attention on the enzymatic structure of laccase.<sup>[85,86]</sup> Laccase is a redox enzyme belonging to the class of multicopper oxidases, which are able to catalyze the reduction of  $O_2$  to  $H_2O$  by exploiting an internal ET (IET) process, hence: (i) electrons donation from an electrode (DET) or freely diffusing/immobilized redox mediators to  $T_1$  copper atom, (ii) IET between  $T_1$  site and  $T_2/T_3$  trinuclear copper cluster, and (iii)  $O_2$  reduction to  $H_2O$ .

Armstrong and co-workers discovered the presence of a hydrophobic pocket in the proximity of the  $T_1$  site rich in  $\pi$  electron density, as shown in Figure 7a, to which a range of organic substrates can bind and undergo rapid, one-electron oxidation to radical products that dissociate before further reaction. In this regard, the authors targeted the hydrophobic pocket by electrodepositing the in situ generated diazonium salt of 2-amino-anthracene ( $Ar-N_2^+$ ). The diazonium salt was deposited by cyclic voltammetry onto a pyrolytic graphite 'edge' (PGE) electrode. The  $Ar-N_2$ -PGE electrode was later modified with *Pycnoporus cinnabarinus* laccase lcc3-1 showing an increased catalytic wave (red curve, Figure 7b) compared to the non-modified electrode (black curve, Figure 7b). The so modified electrode

was stable for up to 60 days. In another report, Minter and co-workers reported a slightly different approach to enhancing the catalytic current of the modified bioelectrode due to enhanced ET rate constant through the enzyme plugging.<sup>[87]</sup> The authors proposed two different synthetic routes to obtain similar compounds, notably 1-pyrenemethyl anthracene-2-carboxylate and 1-pyrenyl anthracene-2-carboxylamide to plug the enzyme through the hydrophobic pocket in both cases. The conjugation of a pyrene group with an anthracene moiety allowed to obtain the  $\pi$ - $\pi$  stacking with nanotubes (pyrene group) and anthracene plugging into the enzyme structure, hence showing an effective immobilization with enzyme orientation. The approach proposed by Armstrong and co-workers were later adopted by Bollella and co-workers to attempt the plugging of a rather bigger enzyme (~150 kDa, bigger than laccase 50–80 kDa), namely FDH,<sup>[88]</sup> that consists of three sub-units: (i) FAD subunit I responsible for the catalytic oxidation of D-fructose to 5-keto-D-fructose, (ii) *heme* subunit II containing three *heme* groups responsible for shuttling the electrons from subunit I to the electrode surface, and (iii) subunit III responsible for the stability of the whole enzyme complex.<sup>[12,89–91]</sup>

Notably, by taking a closer look at the enzyme sequence (unfortunately the crystallographic structure of such enzyme is still not available), it was possible to identify a hydrophobic pocket in the proximity of one of the *heme*



groups (the second one in the sequence). Notably, several groups demonstrated that the third *heme* group is not involved in the ET process being too far apart from the other two (distance longer than 18 Å). The authors clearly succeeded in the isolation of the single *heme* contribution to the total catalytic wave, thus enhancing the ET rate.<sup>[92]</sup>

Despite the investigation of the enzyme structure and sequence, Bartlett and Gorton in a joint project reported the site-specific immobilization of CDH by engineering the enzyme in selected points inserting cysteine groups that would allow for the selective orientation of the enzyme.<sup>[93,94]</sup> Hence, the uniform spatial orientations of CDH influenced DET as follows: (i) orientation of the two-domain enzyme on the side, with cytochrome domain (CYT) in proximity to the electrode, resulted in high DET currents (ii) orientations with a bigger distance between CYT and the electrode, or orientations where CYT could not swing back to the dehydrogenase domain to form the closed enzyme conformation, reduced DET. In the latter case, calcium ions that stabilized the closed conformation of CDH fully recovered DET. Furthermore, a mobile CYT domain can eventually compensate for unfavorable orientations of the catalytic domain to a great extent and allows CDH as a multifactor enzyme to transfer electrons even in awkward orientations. The mobile CYT domain reduces the anisotropy of DET, which is also essential for CDH's physiological function as an extracellular, electron-transferring enzyme.<sup>[94]</sup>

Although many research groups focused on improving the ET rate of several enzymes, the analytical figures of merit of enzyme-based biosensors such as LOD, dynamic linear range, sensitivity, and so forth remain in the micromolar range, thus limiting their exploitation for the development of electrochemical devices toward highly sensitive analytical detection of electroactive and non-electroactive (with enzymatic catalysis) target molecules.

Despite some initial skepticism, the electrochemical community started its transition toward single-molecule electrochemistry by exploiting near-field approaches to achieve the detection of a single molecule directly related to the single ET event. This will be detailed in the next section shedding the light on some limitations of the near field approaches and possible future perspectives.

### 3 | SINGLE-MOLECULE ELECTROCHEMISTRY BY NEAR-FIELD APPROACHES

Single-molecule electrochemistry derives from the Faradaic response of an individual redox molecule in a certain electrochemical environment.<sup>[42,45]</sup> Achieving single-molecule electrochemistry is important mainly

to (i) revisit the fundamental definitions of ET at the molecular scale and the limitations foreseen a long time ago especially considering double-layer structure, mass transport, heterogeneous kinetics, and so forth; (ii) develop electrochemical assays at the individual living cell, where biomarkers amounts are limited to few copies; (iii) perform experiments at nanoscale level confirming the heterogeneities present in a system.<sup>[95]</sup>

Fan and Bard reported the first attempt in 1995, realizing the single-molecule detection by placing a nanometre size electrode in the proximity (nanometre distance) of a counter electrode in a scanning electrochemical microscope apparatus.<sup>[42]</sup> Hence, on average at a concentration of 2 mM, only one molecule should reside in such a small volume ( $\sim 10^{-18}$  cm<sup>3</sup>) between the tip recessed electrode (tip enclosed in a wax insulating layer) and the counter electrode. The ET event would take place in roughly 100 ns generating a Faradaic current in the range of picoamperes. This approach is clearly considered a near-field approach because of the single-molecule confinement. Similarly, Sun and Mirkin reported a glass recessed platinum nanotip that was inserted in a mercury bath in order to create a nanogap geometry able to confine one molecule in a zeptoliter ( $10^{-21}$  L).<sup>[96]</sup>

In both approaches, so far reported, the main drawback is related to the reproducibility of the nanotip electrodes that would dramatically affect the standard deviation on the detection of a single molecule. For this reason, Lemay and co-workers developed a new strategy based on the microfabrication of nanogap through lithography. This approach enables the control of the distance between the electrodes by using a sacrificial layer (an important parameter in redox cycling). First, a three-layer stack consisting of a bottom electrode material, a sacrificial layer (amorphous silicon or chromium), and the top electrode was developed. Once the rest of the device is completed, the sacrificial layer is etched away and replaced with solution, thus creating the nanogap geometry.<sup>[97–100]</sup> The thickness of the sacrificial layer offers the possibility to control the gap between the electrodes, avoiding any possible connection (probably due to heterogeneous sacrificial layer removal) that might short circuit the electrodes. Lemay and co-workers were able to fabricate nanogap electrodes with a spacing of about 50 nm, challenging the process to achieve 20–30 nm, as reported in Figure 8.<sup>[101]</sup> The other main drawback is that the overall concentration involved in a near-field experiment is generally quite a high being at least in the nM range, as it will be addressed later in the text.

The demonstration of single electroactive molecule resolution is a landmark within electrochemistry. Indeed, the nanogaps approach has been widely exploited to detect neurotransmitters at a single-molecule level dur-

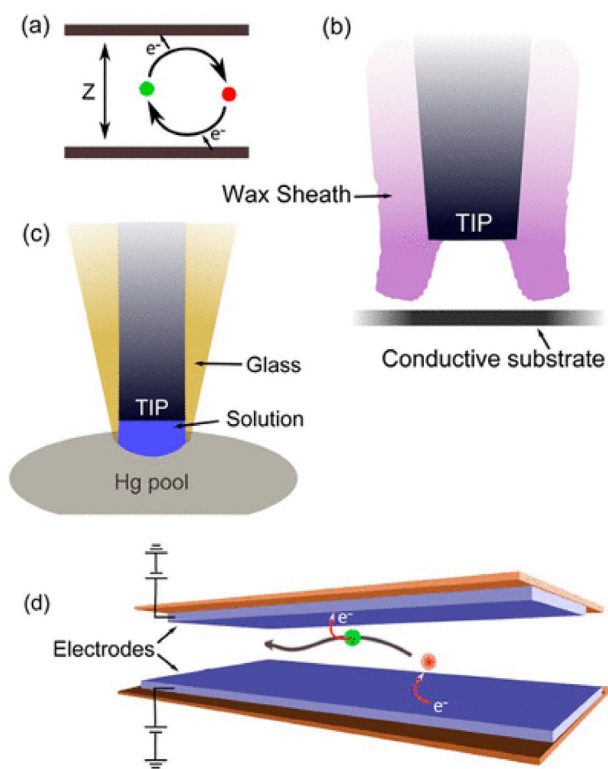


**FIGURE 8** Electrochemical single-molecule detection. (a) The basic concept of redox cycling. (b) Nanoelectrode encased in wax and positioned near a metallic surface. (c) Recessed glass-encased nanoelectrode immersed in mercury. (d) Lithographically fabricated nanogap device. Adopted<sup>[95]</sup> with permission of American Chemical Society (ACS)

ing exocytotic events as reported by Amatore at first, and almost in parallel (a few years later) by Ewing and co-workers.<sup>[102–109]</sup> Since his early career, Amatore and co-workers focused their research on the application of ultramicroelectrodes to monitor sub-second changes in concentrations of neurotransmitters like dopamine, norepinephrine, and serotonin in response to pharmacological and electrical stimuli.<sup>[110,111]</sup> Later, the approach was implemented to detect neurotransmitter release during an individual exocytotic event. Similarly, Ewing used nanotip electrodes to monitor the effect of pharmacological stimuli onto neuronal cells. For instance, he studied the effect of lidocaine on the exocytotic event by combining single-cell amperometry with intracellular vesicle impact electrochemical cytometry.<sup>[109,112–114]</sup>

Besides the single ET at a molecular level, another milestone of single-molecule electrochemistry is the work reported by Turner in 2016 about single enzyme electrochemistry.<sup>[115–117]</sup> This represents an intriguing approach to provide new insight into the ET mechanism at a single enzyme scale. The authors adopted the con-

cept of single-molecule electrochemistry by developing a gold ultramicroelectrode to monitor the electrocatalytic current of a single enzyme entity. In particular, the authors used laccase from *Trametes versicolor*, which, as previously mentioned, uptake the electrons from the electrode surface through the T<sub>1</sub> site that works as an electron relay at a molecular level. Indeed, only when the enzyme molecule is correctly oriented toward the electrode surface, the electrocatalytic current was observed.

Alternatively, Schuhmann and co-workers implemented a system aiming at detecting substrates at a single-cell level as a basis for new analytical devices.<sup>[118–120]</sup> The authors reported the realization of a carbon nanoelectrode by using a highly reproducible etching method different from the previous fabrication of nanogaps in glass nanopores. In particular, the carbon nanofiber was prepared by pyrolytic decomposition of a mixture of butane and propane in a laser-pulled glass capillary. To obtain a protruded carbon nanoelectrode, the glass capillary was etched away by using a buffered solution of fluoridric acid/ammonium fluoride. The carbon nanoelectrode was later modified hexamethylenediamine and polyethylene glycol diglycidyl ether to covalently link an amino-modified osmium redox polymer, acting as a mediator toward glucose oxidation catalyzed by GOx, as schematically displayed in Figure 9.

The so prepared electrode was employed in the continuous monitoring (over 800 s) of glucose levels (in mM range) at the single-cell level.<sup>[119]</sup> Although the innovative approach allows monitoring metabolites at a single-cell level, it does not offer yet the possibility to detect a single substrate molecule, which remains a challenge.

After three decades, there are two open questions: ‘Do we have only statistical limitations?’ and ‘Where do we stand with single-molecule electrochemistry?’. In principle, we should consider that single-molecule electrochemistry cannot be explained solely in terms of Poisson distribution, but we should consider the diffusional barrier that hinders the collision of two molecules into each other and eventually their interaction (enzymatic catalysis) in a reasonably short time when the substrate concentrations are lower than nM. This assumption is valid either if the species are both in solution or one in solution and the other one anchored onto the electrode. Considering a volume of 1  $\mu\text{m}^3$  (corresponding to  $1 \times 10^{-15}$  L), the interaction substrate-enzyme will occur on a minutes scale. To detect a single molecule (i.e.,  $n = 1 \pm 1, \sqrt{n}$ , as Poisson error), one should use the other molecule at nM (i.e.,  $10^{-9}$  M) concentration.<sup>[121]</sup> As suggested above, by inserting a nanometre size electrode in a confined volume, a limited amount of bioreceptors can be hosted on the elec-

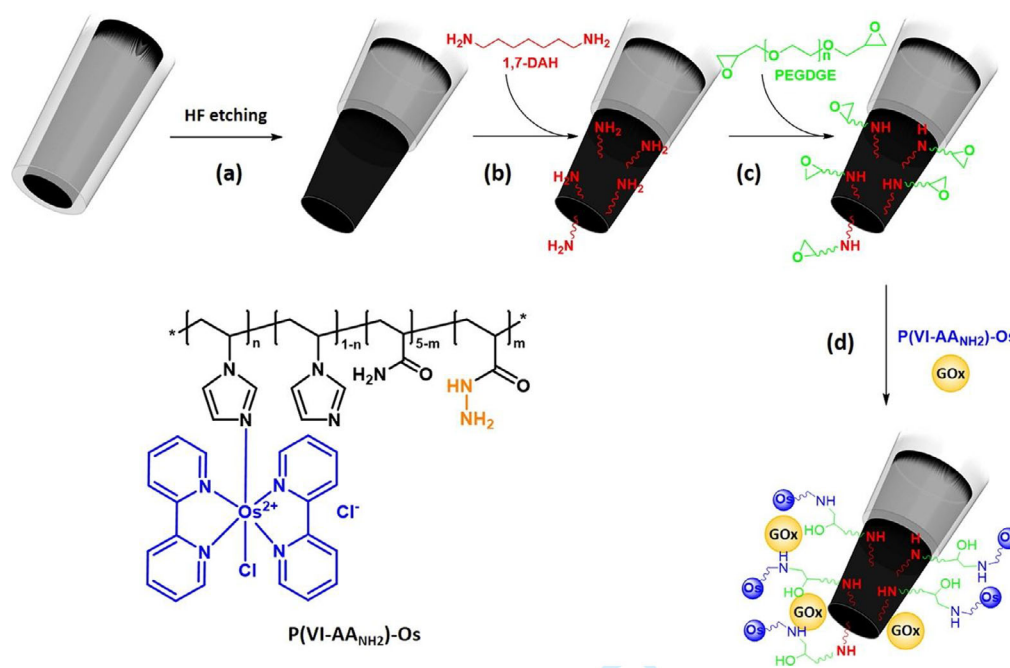


**FIGURE 9** Schematic of the sensor fabrication process (a–d) and molecular structure of the used redox polymer P(VI-AA<sub>NH<sub>2</sub></sub>)-Os. Reproduced<sup>[119]</sup> with permission of Elsevier Ltd

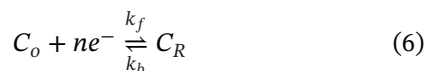
trode surface enabling the ‘virtual’ detection of a single molecule copy considering a high concentration of target analyte ( $\mu\text{M}$  or even  $\text{mM}$ ).<sup>[44,95]</sup> Conversely, considering a  $100\ \mu\text{l}$  sample volume, commonly used in clinical assays, one should consider a wider electrode surface modified with  $10^{11}$ – $10^{12}$  number of bioreceptors (corresponding to  $\text{nM}$  concentration of bioreceptor) to detect the single interaction event in a reasonable time frame.<sup>[121]</sup> This is recalled as a wide-field approach and it has been demonstrated at first by Torsi and co-workers in 2018 considering a millimeter-sized gate electrode integrated into an electrolyte gated field-effect transistor for the immunometric potentiometric detection of the antigenic interaction anti-immunoglobulin G and its cognate antigen (IgG). They succeeded with this approach to detect a single copy of IgG.<sup>[122]</sup> Later, this approach has been reiterated for many biomarkers both antigenic and genomic, with similar performance.<sup>[123–130]</sup> Viruses/antigens at the single-molecule level have been reported also in the development of capacitively coupled organic electrochemical transistors (OECTs).<sup>[131]</sup> Recently, Salleo and co-workers reported the possibility to operate OECTs as an amperometric biosensor by merging a capacitively coupled OECT (amplification cell) with another electrochemical cell where the redox reaction produces a Faradaic current occurs, displaying a current gain up to  $10^3$ .<sup>[132]</sup> Eventually, the possibility that this concept could be transferred to single-molecule electrochemistry is not a mirage.

#### 4 | OVERCOMING THE LIMIT OF DETECTION AT MICROMOLAR LEVEL WITH A WIDE FIELD APPROACH

As previously mentioned, in a wide field approach one should be able to detect a single redox molecule copy in  $100\ \mu\text{l}$  volume by using a wide electrode surface modified with  $10^{11}$ – $10^{12}$  number of biological recognition elements. In this regard, Macchia et al. have theorized the possibility to amplify a small Faradaic current related to an ET process occurring at the electrode surface.<sup>[133]</sup>

As electrochemical systems, we should consider both the electrolytic cell where the application of biasing potential supplies a certain overpotential ( $\eta$ ) with respect to the equilibrium potential ( $E^0$ ) to induce a nonspontaneous redox reaction and the galvanic cell that can produce a certain potential difference ( $\Delta E$ ) as well as current output ( $I_{\text{out}}$ ) using chemical or biochemical reactions catalyzed by inorganic or bio-catalysts (i.e., bacteria, enzymes, etc.).<sup>[134]</sup> In principle, considering a three-electrode electrochemical cell containing working, reference, and counter electrode, to observe the electrolysis of an electroactive molecule (C), one should apply a voltage with respect to a reference electrode to observe a Faradaic current ( $I_F$ ) related to the interfacial ET process. Different from a potentiometric experiment, where the measurement is performed at the equilibrium (no current flowing in the system), the amperometric measurement is performed out of the equi-

librium by applying an external biasing potential so that current can flow in the system to restore the equilibrium. Herein, the applied potential should be always kept constant with respect to a reference electrode (i.e., silver/silver chloride (Ag/AgCl) or saturated calomel electrode).<sup>[135]</sup> The following redox reaction was considered (where C can be assumed as  $\text{Fe}(\text{CN})_6^{3-}$  as the oxidized form undergoing reduction and  $\text{Fe}(\text{CN})_6^{4-}$  like the reduced form undergoing oxidation):



where  $k_f$  ( $\text{cm sec}^{-1}$ ) and  $k_b$  ( $\text{cm sec}^{-1}$ ) are the heterogeneous rate constants for the forward and backward reaction, respectively.

At the equilibrium, the reaction is characterized by the Nernst Equation, being proportional to the concentration of the redox species within the bulk solution:

$$E_C = E_C^0 + \frac{RT}{nF} \ln \frac{C_O^*}{C_R^*} \quad (7)$$

where  $E_C^0$  is the standard equilibrium potential of the redox reaction taking place at the working electrode,  $F$  is Faraday's constant ( $1 F = 96\,485.3 \text{ C mol}^{-1}$ ),  $n$  the number of electrons involved in the faradic process,  $C_j^*$  ( $\text{mol cm}^{-3}$ ) is the bulk concentration for  $C$  either in the reduced or oxidized form, while  $R$  and  $T$  have their usual meaning.

When moving from  $E_C^0$ , applying a certain overpotential  $\eta = E_{\text{appl}} - E_C^0$ , the total current (Faradaic current,  $I_F = i$ ) can be defined as the difference between the cathodic and the anodic current:

$$i = i_c - i_a \quad (8)$$

Both currents are related to the corresponding heterogeneous rate constant:

$$i_c = F A k_f C_O(0, t) \quad (9)$$

$$i_a = F A k_b C_R(0, t) \quad (10)$$

where  $F$  is Faraday's constant,  $A$  ( $\text{cm}^2$ ) is the area of the electrode, and  $C_j(x, t)$  ( $\text{mol cm}^{-3}$ ) is the concentration of species  $j$  at the distance  $x$  ( $\text{cm}$ ) from the electrode the time  $t$  ( $\text{s}$ ). The equation can be written as the ratio between the forward and backward rate constant:

$$k^0 = \frac{k_b}{k_f} = e^{f(E-E^0)} \quad (11)$$

where  $f$  is a factor containing  $(RT/nF)$ . The complete *current-potential characteristic* can be written through the combination of the last equations:

$$i = F A k^0 \left[ C_O(0, t) e^{-\alpha f(E-E^0)} - C_R(0, t) e^{(1-\alpha)f(E-E^0)} \right] \quad (12)$$

where  $\alpha$  is the ET coefficient. This equation is used for every assumption on the heterogeneous electrode kinetics, including the Butler-Volmer equation. At the equilibrium, there is no net current:

$$i_0 = |i_a| = |i_c| \quad (13)$$

where  $i_0$  is the exchange current:

$$i_0 = F A k^0 \quad (14)$$

From the equations the *current-overpotential equation* is defined:

$$i = i_0 \left[ \frac{C_O(0, t)}{C_O^*} e^{-\alpha f \eta} - \frac{C_R(0, t)}{C_R^*} e^{(1-\alpha) f \eta} \right] \quad (15)$$

where  $\eta$  is the overpotential and  $C_j^*$  ( $\text{mol cm}^{-3}$ ) is the bulk concentration for the  $j$  species.

Whenever the potential is applied, the current achieves its highest value (high concentration of electroactive species at the electrode surface), decreasing after the steady-state (electroactive species are consumed at the electrode surface) under diffusion control. In these experimental conditions, the Cottrell equation, derived from Fick's second law, can be used to predict the current trend vs. time. The current is then diffusion controlled. This equation is valid for a planar macroscale electrode:

$$i = \frac{n F A D_O^{1/2} C_O^*}{\pi^{1/2} t^{1/2}} \quad (16)$$

where  $D_O$  ( $\text{cm}^2 \text{ sec}^{-1}$ ) is the diffusion coefficient for  $C$ ,  $F$  is Faraday's constant ( $1F = 96\,485.3 \text{ C mol}^{-1}$ ),  $n$  the number of electrons involved in the faradic process,  $C_O^*$  ( $\text{mol cm}^{-3}$ ) is the bulk concentration for  $C$  and  $A$  ( $\text{cm}^2$ ) is the electrode area. This set of equations can be further rearranged when the electroactive species are immobilized onto the electrode surface.<sup>[136,137]</sup>

To achieve the wide-field single-molecule electrochemistry, a potential solution might be the employment of a BJT, displayed in Figure 10, combined with the enzymatic recycling of an electroactive/non-electroactive molecule operated by  $10^{11}$ – $10^{12}$  enzyme bioreceptors immobilized on



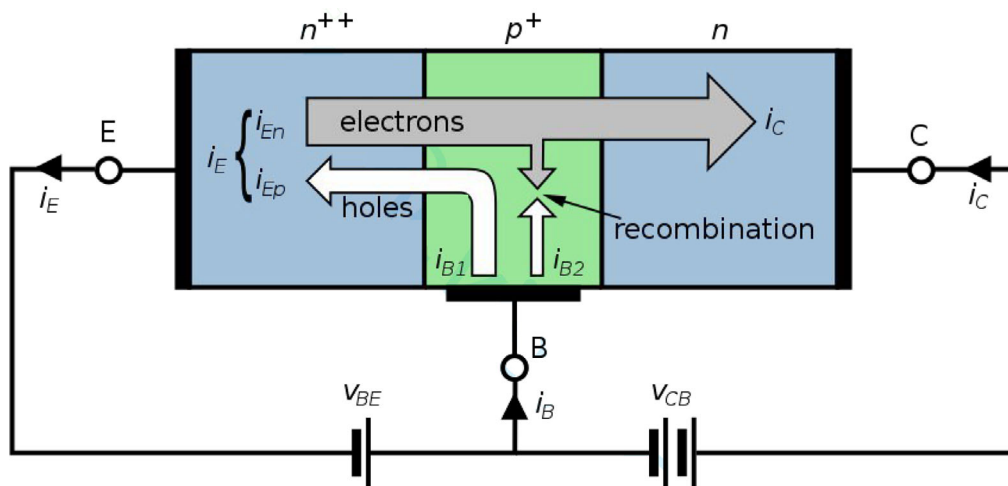


**FIGURE 10** Schematic representation of npn bipolar junction transistor (BJT) and its operation as a current amplifier. Reproduced from [https://en.wikipedia.org/wiki/Bipolar\\_junction\\_transistor#/media/File:NPN\\_BJT\\_Basic\\_Operation\\_\(Active\)\\_jP.svg](https://en.wikipedia.org/wiki/Bipolar_junction_transistor#/media/File:NPN_BJT_Basic_Operation_(Active)_jP.svg) under Commons Creative License 4.0

a millimeter-sized electrode. Indeed, the enzymatic recycling would allow for the detection of a single molecule (conceptually similar to the electrochemical recycling operated in the near-field approach) generating a small current output that is further amplified by a BJT.

BJTs are also regarded as three-terminal devices but with different terminology with respect to the FET. Indeed, in BJT the device terminals are named: Emitter (source), Collector (drain), and Base (gate), alternatively p- or n-doped. By considering a so-called npn BJT, the emitter would be heavily n-doped, the base would be thin and lightly doped while the collector would be n-doped.<sup>[138]</sup> Notoriously, a BJT can be also regarded as two back-to-back diodes. In this regard, we need to consider the formation of two junctions: one n-p between emitter and base (EB) and the other one p-n between base and collector (BC). While operating a BJT, we need to consider that the EB junction is forward biased (positive terminal of the voltage suppliers connected to the p-side of the junction while the negative one is connected to the n-side) while the BC junction is reversed biased.

By injecting holes in the base terminal, they should cross EB junction (forward-biased) where they recombine with electrons (majority charge carriers in the emitter terminal); however, the electrons (the higher amount by several orders of magnitude) due to the forward biasing will be able to cross EB junction undergoing minimal recombination with holes (majority charge carriers in the base terminal) and move forward into the collector terminal by crossing the BC junction that is reversed biased. This will generate an amplified collector current with respect to the base current because  $I_C = \gamma I_B$ , where  $\gamma$  is the amplification

factor (typically  $10^2$ – $10^3$  depending on the BJT).<sup>[133]</sup> At this point, a three-electrode electrochemical cell (also regarded as an electrolytic cell) should be connected as an extended base at the base terminal of the BJT, so that applying a voltage to the working electrode (out of thermodynamic equilibrium) would return an amplified collector current ( $I_C$ ), as follows:

$$I_C = \gamma I_F = \gamma \frac{nFAD_O^{1/2} C_O^*}{\pi^{1/2} t^{1/2}} \quad (17)$$

where all symbols have their usual meaning. In addition, for an enzyme-modified electrode Equation (16) could be reformulated as follows:

$$I_C = \gamma I_{kin} = \gamma \frac{nFA\Gamma k_{cat} [C]}{[C] + K_M} \quad (18)$$

Although it seems straightforward, an electrolytic cell is not able to source out current spontaneously, one would need to apply a voltage bigger than the open circuit potential of the cell to drive a current into the electrochemical cell making the redox reaction occur at the electrode surface. Instead of an electrolytic cell, we should connect a galvanic cell at the base terminal (as extended base configuration) that is able to produce a certain current output proportional to the concentration of the target analyte complying with Equations (16) and (17). This novel approach could potentially pave the way toward the development of highly sensitive amperometric (bio)sensors mathematically demonstrating both the dependence on the target analyte concentration and the existence of an amplification factor.

## 5 | CONCLUSIONS AND FUTURE PERSPECTIVES

Although many researchers within bioelectrochemistry focused their research on enzyme-based amperometric biosensors, we are still far away from achieving sub-nanomolar LOD as well as extending the dynamic linear range over several orders of magnitude (usually one order of magnitude). We highlighted the most representative approaches to enhancing the enzyme loading and increasing the ET rate constant. In both cases, we should acknowledge as the introduction of nanomaterials like both carbon- and metal-based nanomaterials onto an electrode surface dramatically increases the enzyme loading.<sup>[139]</sup> However, we are still in the micromolar range with all analytical figures of merit, sometimes in the nanomolar range.<sup>[140]</sup> Also, single-molecule electrochemistry has been widely exploited as a proof-of-concept for the detection of the single ET event, later practically exploited for the detection of neurotransmitters released by the neuronal cell during exocytotic events.<sup>[103,114]</sup> In addition, other researchers tried to implement single enzyme bioelectrocatalysis but are still far from being a Point-of-Care (PoC) device. Also, OECTs detecting Faradaic reactions have been shown to work at most in the nM range.<sup>[141–143]</sup>

From a future perspective, we discussed the possibility to implement a BJT in an extended base configuration connected with an electrochemical cell, where the sensing operation is occurring. This approach was partially inspired by the mechanism exploited in the near-field single-molecule electrochemistry, where the redox species recycling in a tiny volume (nanometre size, with volumes as low as  $10^{-18}$ – $10^{-21}$  L) is important to record single ET events usually occurring in nanosecond intervals. In BJT extended base configuration, we would need to amplify the Faradaic current derived from a single ET event but exploiting this time biochemical recycling performed by  $10^{11}$ – $10^{12}$  bioreceptors immobilized onto a millimeter-sized electrode in a volume of 100  $\mu$ l, which is suitable for the development of PoC devices. This intriguing approach could open many avenues for the development of new kinds of bioelectronics (notably, based on electrochemistry and transistor technology) for ultrasensitive sensing of the electroactive molecule at a single-molecule level defined as a wide-field approach.

### ACKNOWLEDGMENTS

The following funding agencies are acknowledged: Academy of Finland projects #316881, #316883 “Spatiotemporal control of Cell Functions”, #332106 “ProSiT—Protein Detection at the Single-Molecule Limit with a Self-powered Organic Transistor for HIV early diagnosis”; Biosensori analitici usa-e getta a base di transistori

organici auto-alimentati per la rivelazione di biomarcatori proteomici alla singola molecola per la diagnostica decentrata dell’HIV (6CDD3786); Research for Innovation REFIN—Regione Puglia POR PUGLIA FESR-FSE 2014–2020; Dottorati innovativi con caratterizzazione industriale—PON R&I 2014–2020; “Sensore bio-elettronico usa-e-getta per l’HIV autoalimentato da una cella a combustibile biologica” (BioElSens&Fuel); SiMBiT—Single molecule bio-electronic smart system array for clinical testing (Grant agreement ID: 824946); PMGB—Sviluppo di piattaforme meccatroniche, genomiche e bioinformatiche per l’oncologia di precisione—ARS01\_01195-PON “RICERCA E INNOVAZIONE” 2014–2020; Åbo Akademi University CoE “Bioelectronic activation of cell functions”; and CSGI are acknowledged for partial financial support.

### AUTHOR CONTRIBUTIONS

All authors have thoroughly contributed to conceiving and writing this article. The final version was approved by all authors.

### CONFLICT OF INTEREST

The authors declare no conflict of interest.

### DATA AVAILABILITY STATEMENT

Not applicable.

### ORCID

Paolo Bollella  <https://orcid.org/0000-0001-9049-6406>

### REFERENCES

1. P. Bollella, L. Gorton, *Curr. Opin. Electrochem.* **2018**, *10*, 157.
2. P. Bollella, E. Katz, *Sensors* **2020**, *20*, 3517.
3. J. Kim, A. S. Campbell, B. E. -F. de Ávila, J. Wang, *Nat. Biotechnol.* **2019**, *37*, 389.
4. J. Min, J. R. Sempionatto, H. Teymourian, J. Wang, W. Gao, *Biosens. Bioelectron.* **2021**, *172*, 112750.
5. E. Battista, V. Lettera, M. Villani, D. Calestani, F. Gentile, P. A. Netti, S. Iannotta, A. Zappettini, N. Coppede, *Org. Electron.* **2017**, *40*, 51.
6. P. Bollella, L. Gorton, R. Antiochia, *Sensors* **2018**, *18*, 1319.
7. L. C. Clark, C. Lyons, *Ann. N. Y. Acad. Sci.* **1962**, *102*, 29.
8. A. A. Karyakin, O. V. Gitelmacher, E. E. Karyakina, *Anal. Chem.* **1995**, *67*, 2419.
9. A. A. Karyakin, E. E. Karyakina, W. Schuhmann, H. -L. Schmidt, S. D. Varfolomeyev, *Electroanalysis* **1994**, *6*, 821.
10. A. A. Karyakin, O. A. Bobrova, E. E. Karyakina, *J. Electroanal. Chem.* **1995**, *399*, 179.
11. E. Katz, T. Lötzbeyer, D. D. Schlereth, W. Schuhmann, H. -L. Schmidt, *J. Electroanal. Chem.* **1994**, *373*, 189.
12. T. Adachi, Y. Kitazumi, O. Shirai, K. Kano, *Catalysts* **2020**, *10*, 236.
13. A. L. Ghindilis, P. Atanasov, E. Wilkins, *Electroanalysis* **1997**, *9*, 661.

14. J. F. Rusling, Z. Zhang, *Handbook of Surfaces and Interfaces of Materials*, Elsevier, Amsterdam, NL **2001**.
15. W. Zhang, G. Li, *Anal. Sci.* **2004**, *20*, 603.
16. Y. Wu, S. Hu, *Microchim. Acta* **2007**, *159*, 1.
17. R. A. Marcus, *Angew. Chem., Int. Ed. Engl.* **1993**, *32*, 1111.
18. R. A. Marcus, *Annu. Rev. Phys. Chem.* **1964**, *15*, 155.
19. R. A. Marcus, *J. Chem. Phys.* **1956**, *24*, 966.
20. R. A. Marcus, *Faraday Discuss. Chem. Soc.* **1982**, *74*, 7.
21. R. A. Marcus, *J. Phys. Chem.* **1963**, *67*, 853.
22. M. Tachiya, *J. Phys. Chem.* **1993**, *97*, 5911.
23. A. I. Yaropolov, I. V. Berezin, *Russ. Chem. Rev.* **1985**, *54*, 852.
24. S. D. Varfolomeev, I. N. Kurochkin, A. I. Yaropolov, *Biosens. Bioelectron.* **1996**, *11*, 863.
25. A. I. Yaropolov, O. V. Skorobogat'Ko, S. S. Vartanov, S. D. Varfolomeyev, *Appl. Biochem. Biotechnol.* **1994**, *49*, 257.
26. D. Ivniński, B. Branch, P. Atanassov, C. Apblett, *Electrochem. Commun.* **2006**, *8*, 1204.
27. S. Shleev, A. Jarosz-Wilkolazka, A. Khalunina, O. Morozova, A. Yaropolov, T. Ruzgas, L. Gorton, *Bioelectrochemistry* **2005**, *67*, 115.
28. R. Ortiz, H. Matsumura, F. Tascia, K. Zahma, M. Samejima, K. Igarashi, R. Ludwig, L. Gorton, *Anal. Chem.* **2012**, *84*, 10315.
29. A. Killyéni, M. E. Yakovleva, D. MacAodha, P. Ó. Conghaile, C. Gonaus, R. Ortiz, D. Leech, I. C. Popescu, C. K. Peterbauer, L. Gorton, *Electrochimica Acta* **2014**, *126*, 61.
30. Y. Xiao, F. Patolsky, E. Katz, J. F. Hainfeld, I. Willner, *Science* **2003**, *299*, 1877.
31. R. Wilson, A. P. F. Turner, *Biosens. Bioelectron.* **1992**, *7*, 165.
32. G. S. Wilson, *Biosens. Bioelectron.* **2016**, *82*, vii.
33. M. Wooten, S. Karra, M. Zhang, W. Gorski, *Anal. Chem.* **2014**, *86*, 752.
34. P. N. Bartlett, F. A. Al-Lolage, *J. Electroanal. Chem.* **2018**, *819*, 26.
35. P. Bollella, *Nanomaterials* **2020**, *10*, 722.
36. P. Bollella, E. Katz, *Methods Enzymol.* **2020**, *630*, 215.
37. S. Zhao, F. Caruso, L. Dähne, G. Decher, B. G. De Geest, J. Fan, N. Feliu, Y. Gogotsi, P. T. Hammond, M. C. Hersam, *ACS Nano* **2019**, *13*, 6151.
38. S. C. Feifel, F. Lisdat, *J. Nanobiotechnol.* **2011**, *9*, 59.
39. F. Mazzei, G. Favero, P. Bollella, C. Tortolini, L. Mannina, M. E. Conti, R. Antiochia, *Int. J. Environ. Health* **2015**, *7*, 267.
40. U. Hanefeld, L. Gardossi, E. Magner, *Chem. Soc. Rev.* **2009**, *38*, 453.
41. R. A. Sheldon, S. van Pelt, *Chem. Soc. Rev.* **2013**, *42*, 6223.
42. F. -R. F. Fan, A. J. Bard, *Science* **1995**, *267*, 871.
43. Y. Fan, T. J. Anderson, B. Zhang, *Curr. Opin. Electrochem.* **2018**, *7*, 81.
44. A. J. Bard, *ACS Nano* **2008**, *2*, 2437.
45. A. J. Bard, F. -R. F. Fan, *Acc. Chem. Res.* **1996**, *29*, 572.
46. S. Karra, W. Gorski, *Anal. Chem.* **2013**, *85*, 10573.
47. S. V. Dzyadevych, V. N. Arkhypova, A. P. Soldatkin, A. V. El'Skaya, C. Martelet, N. Jaffrezic-Renault, *Irbm* **2008**, *29*, 171.
48. F. Scheller, D. Kirstein, L. Kirstein, F. Schubert, U. Wollenberger, B. Ollson, L. Gorton, G. Johansson, *Philos. Trans. R. Soc. Lond. B Biol. Sci.* **1987**, *316*, 85.
49. A. Riklin, E. Katz, I. Wiliner, A. Stocker, A. F. Bückmann, *Nature* **1995**, *376*, 672.
50. A. Lindgren, T. Ruzgas, L. Gorton, E. Csöregi, G. B. Ardila, I. Y. Sakharov, I. G. Gazaryan, *Biosens. Bioelectron.* **2000**, *15*, 491.
51. O. Smutok, T. Kavetsky, E. Katz, *Curr. Opin. Electrochem.* **2021**, art. No. 100856, <https://doi.org/10.1016/j.coelec.2021.100856>.
52. M. Kizling, R. Bilewicz, *ChemElectroChem* **2018**, *5*, 166.
53. F. J. Vidal-Iglesias, J. Solla-Gullón, V. Montiel, A. Aldaz, *Electrochem. Commun.* **2012**, *15*, 42.
54. E. G. Michael, *Analyst* **1996**, *121*, 715.
55. G. L. Atkins, I. A. Nimmo, *Anal. Biochem.* **1980**, *104*, 1.
56. H. A. Heering, M. S. Mondal, F. A. Armstrong, *Anal. Chem.* **1999**, *71*, 174.
57. X. Xiao, P. Si, E. Magner, *Bioelectrochemistry* **2016**, *109*, 117.
58. T. Siepenkoetter, U. Salaj-Kosla, X. Xiao, S. Belochapkin, E. Magner, *Electroanalysis* **2016**, *28*, 2415.
59. M. D. Angione, R. Pilolli, S. Cotrone, M. Magliulo, A. Mallardi, G. Palazzo, L. Sabbatini, D. Fine, A. Dodabalapur, N. Cioffi, *Mater. Today* **2011**, *14*, 424.
60. N. Iqbal, A. Afzal, N. Cioffi, L. Sabbatini, L. Torsi, *Sens. Actuators B Chem.* **2013**, *181*, 9.
61. M. Trojanowicz, *TrAC Trends Anal. Chem.* **2006**, *25*, 480.
62. M. D. Rubianes, G. A. Rivas, *Electroanalysis* **2005**, *17*, 73–78.
63. L. Agüí, P. Yáñez-Sedeño, J. M. Pingarrón, *Anal. Chim. Acta* **2008**, *622*, 11–47.
64. A. Sassolas, L. J. Blum, B. D. Leca-Bouvier, *Biotechnol. Adv.* **2012**, *30*, 489–511.
65. P. Bollella, G. Fusco, C. Tortolini, G. Sanzò, G. Favero, L. Gorton, R. Antiochia, *Biosens. Bioelectron.* **2017**, *89*, 152–166.
66. P. Bollella, G. Fusco, D. Stevar, L. Gorton, R. Ludwig, S. Ma, H. Boer, A. Koivula, C. Tortolini, G. Favero, R. Antiochia, F. Mazzei, *Sens. Actuators B Chem.* **2018**, *256*, 921–930.
67. F. Lisdat, *Biosensing for the 21st Century*, Springer, Switzerland **2007**.
68. F. Lisdat, *Curr. Opin. Electrochem.* **2017**, *5*, 165–172.
69. F. Lisdat, *J. Solid State Electrochem.* **2020**, *24*, 2125–2127.
70. M. Grattieri, S. D. Minter, *ACS Sens.* **2018**, *3*, 44–53.
71. F. C. Macazo, S. D. Minter, *Curr. Opin. Electrochem.* **2017**, *5*, 114–120.
72. V. Fourmond, C. Léger, *Curr. Opin. Electrochem.* **2017**, *1*, 110–120.
73. L. P. Jenner, J. N. Butt, *Curr. Opin. Electrochem.* **2018**, *8*, 81–88.
74. L. Qian, X. Yang, *Talanta* **2006**, *68*, 721–727.
75. W. -C. Wu, J. -L. Huang, Y. -C. Tsai, *Mater. Sci. Eng. C* **2012**, *32*, 983–987.
76. P. Vatsyayan, S. Bordoloi, P. Goswami, *Biophys. Chem.* **2010**, *153*, 36–42.
77. G. Fusco, P. Bollella, F. Mazzei, G. Favero, R. Antiochia, C. Tortolini, *J. Anal. Methods Chem.* **2016**, *2016*, 1.
78. P. Vatsyayan, M. Chakraborty, S. Bordoloi, P. Goswami, *J. Electroanal. Chem.* **2011**, *662*, 312–316.
79. S. R. Chinnadayala, A. Kakoti, M. Santhosh, P. Goswami, *Biosens. Bioelectron.* **2014**, *55*, 120–126.
80. M. Das, P. Goswami, *Bioelectrochemistry* **2013**, *89*, 19–25.
81. J. J. Gooding, R. Wibowo, J. Liu, W. Yang, D. Losic, S. Orbons, F. J. Mearns, J. G. Shapter, D. B. Hibbert, *J. Am. Chem. Soc.* **2003**, *125*, 9006–9007.
82. M. Tavahodi, R. Ortiz, C. Schulz, A. Ekhtiari, R. Ludwig, B. Haghighi, L. Gorton, *ChemPlusChem* **2017**, *82*, 546–552.
83. P. Bollella, Y. Hibino, K. Kano, L. Gorton, R. Antiochia, *Anal. Chem.* **2018**, *90*, 12131–12136.
84. F. Patolsky, Y. Weizmann, I. Willner, *Angew. Chem.* **2004**, *43*, 2113–2117.

85. F. A. Armstrong, *Curr. Opin. Chem. Biol.* **2005**, *9*, 110–117.
86. C. F. Blanford, R. S. Heath, F. A. Armstrong, *Chem. Commun.* **2007**, 1710–1712.
87. F. Giroud, S. D. Minter, *Electrochem. Commun.* **2013**, *34*, 157–160.
88. P. Bollella, Y. Hibino, K. Kano, L. Gorton, R. Antiochia, *ACS Catal.* **2018**, *8*, 10279–10289.
89. T. Adachi, Y. Kitazumi, O. Shirai, K. Kano, *Sensors* **2020**, *20*, 4826.
90. P. Bollella, Y. Hibino, K. Kano, L. Gorton, R. Antiochia, *Anal. Bioanal. Chem.* **2018**, *410*, 3253–3264.
91. P. Bollella, Y. Hibino, P. Conejo-Valverde, J. Soto-Cruz, J. Bergueiro, M. Calderón, O. Rojas-Carrillo, K. Kano, L. Gorton, *Anal. Bioanal. Chem.* **2019**, *411*, 7645–7657.
92. P. Bollella, Z. Boeva, R. -M. Latonen, K. Kano, L. Gorton, J. Bobacka, *Biosens. Bioelectron.* **2021**, *176*, 112909.
93. M. Meneghello, F. A. Al-Lolage, S. Ma, R. Ludwig, P. N. Bartlett, *ChemElectroChem* **2019**, *6*, 700–713.
94. S. Ma, C. V. Laurent, M. Meneghello, J. Tuoriniemi, C. Oostenbrink, L. Gorton, P. N. Bartlett, R. Ludwig, *ACS Catal.* **2019**, *9*, 7607–7615.
95. S. G. Lemay, S. Kang, K. Mathwig, P. S. Singh, *Acc. Chem. Res.* **2013**, *46*, 369–377.
96. P. Sun, M. V. Mirkin, *J. Am. Chem. Soc.* **2008**, *130*, 8241–8250.
97. S. Kang, A. F. Nieuwenhuis, K. Mathwig, D. Mampallil, S. G. Lemay, *ACS Nano* **2013**, *7*, 10931–10937.
98. K. Mathwig, S. G. Lemay, *Electrochim. Acta* **2013**, *112*, 943–949.
99. K. Mathwig, T. J. Aartsma, G. W. Canters, S. G. Lemay, *Annu. Rev. Anal. Chem.* **2014**, *7*, 383–404.
100. S. Kang, A. F. Nieuwenhuis, K. Mathwig, D. Mampallil, Z. A. Kostichenko, S. G. Lemay, *Faraday Discuss.* **2016**, *193*, 41–50.
101. H. R. Zafarani, K. Mathwig, E. J. Sudhölter, L. Rassaei, *J. Electroanal. Chem.* **2016**, *760*, 42–47.
102. C. Amatore, S. Arbault, D. Bruce, P. de Oliveira, M. Erard, M. Vuillaume, *Chem. Eur. J.* **2001**, *7*, 4171–4179.
103. C. Amatore, S. Arbault, M. Guille, F. Lemaître, *Chem. Rev.* **2008**, *108*, 2585–2621.
104. S. Arbault, P. Pantano, N. Sojic, C. Amatore, M. Best-Belpomme, A. Sarasin, M. Vuillaume, *Carcinogenesis* **1997**, *18*, 569–574.
105. M. R. Filipović, A. C. Koh, S. Arbault, V. Niketić, A. Debus, U. Schleicher, C. Bogdan, M. Guille, F. Lemaître, C. Amatore, *Angew. Chem.* **2010**, *122*, 4324–4328.
106. M. K. Passarelli, A. G. Ewing, *Curr. Opin. Chem. Biol.* **2013**, *17*, 854–859.
107. C. Gu, X. Zhang, A. G. Ewing, *Anal. Chem.* **2020**, *92*, 10268–10273.
108. X. Li, J. Dunevall, A. G. Ewing, *Angew. Chem.* **2016**, *128*, 9187–9190.
109. B. Zhang, K. L. Adams, S. J. Luber, D. J. Eves, M. L. Heien, A. G. Ewing, *Anal. Chem.* **2008**, *80*, 1394–1400.
110. C. Amatore, Y. Bouret, E. R. Travis, R. M. Wightman, *Biochimie* **2000**, *82*, 481–496.
111. C. Amatore, Y. Bouret, E. R. Travis, R. M. Wightman, *Angew. Chem. Int. Ed.* **2000**, *39*, 1952–1955.
112. X. Li, A. S. Mohammadi, A. G. Ewing, *J. Electroanal. Chem.* **2016**, *781*, 30–35.
113. Y. Lin, R. Trouillon, M. I. Svensson, J. D. Keighron, A. -S. Cans, A. G. Ewing, *Anal. Chem.* **2012**, *84*, 2949–2954.
114. R. Trouillon, A. G. Ewing, *Anal. Chem.* **2013**, *85*, 4822–4828.
115. A. N. Sekretaryova, M. Y. Vagin, A. P. Turner, M. Eriksson, *J. Am. Chem. Soc.* **2016**, *138*, 2504–2507.
116. C. Davis, S. X. Wang, L. Sepunaru, *Curr. Opin. Electrochem.* **2021**, *25*, 100643.
117. E. Kätelhön, L. Sepunaru, A. A. Karyakin, R. G. Compton, *ACS Catal.* **2016**, *6*, 8313–8320.
118. M. Marquitan, M. D. Mark, A. Ernst, A. Muhs, S. Herlitzte, A. Ruff, W. Schuhmann, *J. Mater. Chem. B* **2020**, *8*, 3631–3639.
119. M. Marquitan, A. Ruff, M. Bramini, S. Herlitzte, M. D. Mark, W. Schuhmann, *Bioelectrochemistry* **2020**, *133*, 107487.
120. J. Clausmeyer, W. Schuhmann, *TrAC Trends Anal. Chem.* **2016**, *79*, 46–59.
121. E. Macchia, K. Manoli, C. Di Franco, G. Scamarcio, L. Torsi, *Anal. Bioanal. Chem.* **2020**, *412*, 5005–5014.
122. E. Macchia, K. Manoli, B. Holzer, C. Di Franco, M. Ghittorelli, F. Torricelli, D. Alberga, G. F. Mangiatordi, G. Palazzo, G. Scamarcio, *Nat. Commun.* **2018**, *9*, art. No. 3223.
123. E. Macchia, P. Romele, K. Manoli, M. Ghittorelli, M. Magliulo, Z. M. Kovács-Vajna, F. Torricelli, L. Torsi, *Flex. Print. Electron.* **2018**, *3*, 034002.
124. E. Macchia, K. Manoli, C. Di Franco, R. A. Picca, R. Österbacka, G. Palazzo, F. Torricelli, G. Scamarcio, L. Torsi, *ACS Sens.* **2020**, *5*, 1822–1830.
125. R. A. Picca, K. Manoli, E. Macchia, L. Sarcina, C. Di Franco, N. Cioffi, D. Blasi, R. Österbacka, F. Torricelli, G. Scamarcio, L. Torsi, *Adv. Funct. Mater.* **2020**, *30*, 1904513.
126. S. K. Sailapu, E. Macchia, I. Merino-Jimenez, J. P. Esquivel, L. Sarcina, G. Scamarcio, S. D. Minter, L. Torsi, N. Sabaté, *Biosens. Bioelectron.* **2020**, *156*, 112103.
127. L. Sansone, E. Macchia, C. Taddei, L. Torsi, M. Giordano, *Sens. Actuators B Chem.* **2018**, *255*, 1097–1104.
128. B. Holzer, K. Manoli, N. Ditaranto, E. Macchia, A. Tiwari, C. Di Franco, G. Scamarcio, G. Palazzo, L. Torsi, *Adv. Biosyst.* **2017**, *1*, 1700055.
129. F. Torricelli, D. Z. Adrahtas, Z. Bao, M. Berggren, F. Biscarini, A. Bonfiglio, C. A. Bortolotti, C. D. Frisbie, E. Macchia, G. G. Malliaras, I. McCulloch, M. Moser, T. -Q. Nguyen, R. M. Owens, A. Salleo, A. Spanu, L. Torsi, *Nat. Rev. Methods Primer* **2021**, *1*, art. No. 66.
130. E. Macchia, A. Tiwari, K. Manoli, B. Holzer, N. Ditaranto, R. A. Picca, N. Cioffi, C. Di Franco, G. Scamarcio, G. Palazzo, L. Torsi, *Chem. Mater.* **2019**, *31*, 6476–6483.
131. K. Guo, S. Wustoni, A. Koklu, E. Díaz-Galicia, M. Moser, A. Hama, A. A. Alqahtani, A. N. Ahmad, F. S. Alhamlan, M. Shuaib, A. Pain, I. McCulloch, S. T. Arold, R. Grünberg, S. Inal, *Nat. Biomed. Eng.* **2021**, 666–677.
132. S. T. M. Tan, A. Giovannitti, A. Melianas, M. Moser, B. L. Cotts, D. Singh, I. McCulloch, A. Salleo, *Adv. Funct. Mater.* **2021**, *31*, 2010868.
133. E. Macchia, R. A. Picca, K. Manoli, C. Di Franco, D. Blasi, L. Sarcina, N. Ditaranto, N. Cioffi, R. Österbacka, G. Scamarcio, F. Torricelli, L. Torsi, *Mater. Horiz.* **2020**, *7*, 999–1013.
134. E. Katz, P. Bollella, *Isr. J. Chem.* **2021**, *61*, 68–84.
135. A. J. Bard, L. R. Faulkner, *Electrochem. Methods* **2001**, *2*, 580–632.
136. C. Léger, A. K. Jones, S. P. Albracht, F. A. Armstrong, *J. Phys. Chem. B* **2002**, *106*, 13058–13063.
137. Q. Chi, J. Zhang, P. S. Jensen, H. E. Christensen, J. Ulstrup, *Faraday Discuss.* **2006**, *131*, 181–195.



138. S. M. Sze, Y. Li, K. K. Ng, *Physics of Semiconductor Devices*, John Wiley & Sons, New York **2021**.
139. H. Li, S. Liu, Z. Dai, J. Bao, X. Yang, *Sensors* **2009**, *9*, 8547–8561.
140. F. W. Scheller, U. Wollenberger, A. Warsinke, F. Lisdat, *Curr. Opin. Biotechnol.* **2001**, *12*, 35–40.
141. D. A. Bernards, D. J. Macaya, M. Nikolou, J. A. DeFranco, S. Takamatsu, G. G. Malliaras, *J. Mater. Chem.* **2008**, *18*, 116–120.
142. A. M. Pappa, D. Ohayon, A. Giovannitti, I. P. Maria, A. Savva, I. Uguz, J. Rivnay, I. McCulloch, R. M. Owens, S. Inal, *Sci. Adv.* **2018**, *4*, art. No. eaat0911.
143. D. Ohayon, G. Nikiforidis, A. Savva, A. Giugni, S. Wustoni, T. Palanisamy, X. Chen, I. P. Maria, E. Di Fabrizio, P. M. Costa, *Nat. Mater.* **2020**, *19*, 456–463.

## AUTHOR BIOGRAPHIES



**Luisa Torsi** is a Professor of chemistry at the University of Bari and an Adjunct Professor at Abo Academy University. She received her Laurea degree in Physics and PhD in Chemical Sciences from UNIBA and was a post-doctoral fellow at Bell Labs in the USA. She was the first woman awarded the

H. E. Merck prize. She was also awarded the Distinguished Women Award by the International Union of Pure and Applied Chemistry. Lately, she was awarded also the Wilhelm Exner Medal 2021. Torsi has authored almost 220 ISI papers, including papers published in *Science*, *Nature Materials*. Her works gathered almost 14,000 Google scholar citations resulting in an h-index of 56. Gathered research funding for over 26 M€, comprises several European and national contracts. Torsi is committed to role model for younger women scientists. In a recent campaign, she was featured in a story of TOPOLINO (Italian comic digest-size series of Disney comics), as “Louise Torduck”, a successful female scientist of the Calisota valley.



**Paolo Bollella** is an Assistant Professor at the University of Bari in the Department of Chemistry. Till December 2020, he was a Research Assistant Professor at Clarkson University in the Department of Chemistry and Biomolecular Science (USA). After his PhD, he joined the

Department of Analytical Chemistry at Åbo Akademi in Turku (Finland) with a Johan Gadolin PostDoc fellowship awarded from the board of Johan Gadolin Process Chemistry Center. In October 2018, he joined the group of “Bioelectronics & Bionanotechnology” led by Professor Evgeny Katz. In March 2019, he was awarded the Minerva Prize for the Scientific Research – Merit Mention for the achievements obtained during his doctoral thesis based on the study of Mediated/Direct Electron Transfer of Redox Protein for Biosensors and Biofuel Cells Applications. In 2020, he was recognized among the top 100,000 most influencing scientists and engineers (statistical analysis elaborated by Stanford University). He is the author of 72 papers on peer-reviewed international journals (Hirsch-index 20), three book chapters, one student book, two proceedings, and almost 60 oral or poster contributions to national and international conferences.

**How to cite this article:** A. Tricase, A. Imbriano, E. Macchia, L. Sarcina, C. Scandurra, F. Torricelli, N. Cioffi, L. Torsi, P. Bollella, *Electrochem. Sci. Adv.* **2023**, *3*, e2100215.

<https://doi.org/10.1002/elsa.202100215>